Micro-Doppler Characteristics of mmWave Indoor Backscattering Channels for RF Sensing

Nurilla Avazov, Rym Hicheri, and Matthias Pätzold,
Faculty of Engineering and Science, University of Agder, P.O.Box 509, 4898 Grimstad, Norway
E-mails: {nurilla.avazov, rym.hicheri, matthias.paetzold}@uia.no

***Abstract*—In indoor environments, backscattering components play a key role in radio-frequency (RF) sensing, especially with the blockage of line-of-sight components by the furniture. Thus, it is paramount to investigate the Doppler characteristics of backscattering millimeter wave (mmWave) channels in the presence of moving objects. In this regard, this paper presents a trajectory-driven non-stationary channel model for a mmWave single-input single-output communication system. This backscattering channel model takes into account the impact of a single moving object on the indoor radio wave propagation phenomena. First, the expression of the complex channel gain is presented. Then, the time-variant (TV) micro-Doppler signatures of the moving object are studied. The validity of the proposed channel model is confirmed by real-world measured RF data, which were collected in a laboratory room using a software defined radar system operating at 24 GHz. For fair comparison, we consider as a moving object a swinging pendulum for which the exact TV trajectory is known. In addition, inertial measurement unit sensors are attached to the pendulum to track its TV trajectory. A good agreement can be seen between the Doppler characteristics of the backscattering channel model and those computed from the measured RF data. This demonstrates that backscattering components can be employed to accurately extract the micro-Doppler signatures of a moving object in indoor spaces. The exhibited results can serve as a basis for the development of future robust backscattering-based RF sensing.**

***Index Terms*—Backscattering, micro-Doppler signatures, millimeter wave communications, non-stationary indoor channels.**

I. Introduction

A common assumption in radio communications is that backscattering can be neglected due to the low power of the received radio-frequency (RF) signals, when analysing the micro-Doppler signatures of a moving object. This assumption can be challenged in the case of RF sensing applications in indoor environments, which are heavily furnished resulting in blockage of line-of-sight (LOS) components. This is best exemplified by the comparative study conducted in [1], where the scattering process analysis and identification was presented by using measured millimeter wave (mmWave) channel properties in a typical conference room. This study resulted in the identification of dominant scattering components, such as LOS, single- and double-bounce scattering (backscattering) components. This puts emphasis on the importance of investigating the contribution and leveraging of backscattering components in indoor spaces for RF sensing.

For this reason, backscattering communications have recently attracted great attention from both research institutes and industries thanks to the pervasive connectivity of power efficient and cost efficient wireless devices [2]. For example, for Internet of Things (IoT) applications exploiting backscattering communications is becoming a promising solution that can enable LOS-like communication channel links for ensuring reliable and robust RF sensing technologies.

In the literature, there exist several studies reporting the impact of multipath radio wave propagation considering the contributions of backscattering components to the channel characteristics using different RF sensing technologies. For instance, the signal propagation from semi-passive RF sensor nodes to an frequency-modulated continuous wave (FMCW) radar was examined for simultaneous ranging in [3]. In this work, the measurements were conducted in a cluttered (furnished) indoor environment using S-band radar operating at center frequency of 2.45 GHz. Other measurement campaigns for the characterization of the delay spread of mmWave indoor backscattering channels can be found in [4]. In [5], the parameterization of diffuse models, namely, the directive and the Lambertian models, was presented considering the impact of different reflecting materials. Model parameters were computed by performing a comparison analysis between the simulation results and measurements conducted at 60 GHz frequency. An example of backscattering communications using WiFi signals can be found in [6]. Moreover, the impact of correlation properties between backscattering and forward channel links on the symbol error rate was analyzed in [7] considering diversity systems over Nakagami-m fading channels. In [8], RF identification was investigated based on distributed passive backscattering systems. Recently, Luo *et al.* presented the TagLoc system that uses off-the-shelf Intel 5300 WiFi cards and enables device-to-device localization [9].

In accordance with the aforementioned research works, there is a great need for a fundamental understanding of the Doppler properties of non-stationary indoor backscattering channels in the presence of a moving object. Therefore, we propose in this paper a trajectory-driven three-dimensional (3D) mmWave non-stationary backscattering channel model, which incorporates the mobility of a moving object (modelled by a single point scatterer) in indoor spaces. Our aim is to demonstrate that the Doppler properties of the underlying channel can be solely extracted from the backscattering components, which can later be used for future RF sensing solutions. For thorough analysis of leveraging backscattering components, we consider a scenario

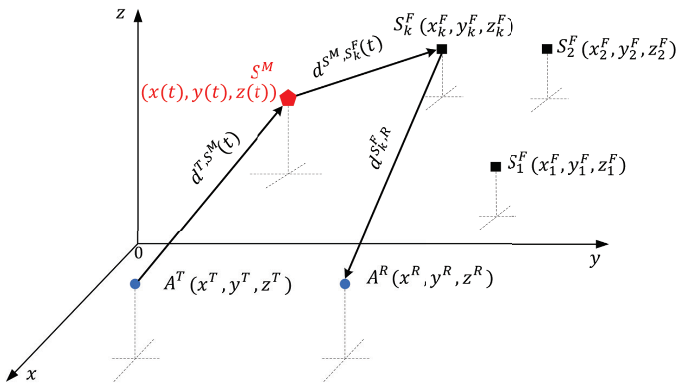

Fig. 1. Illustration of 3D geometrical model for SISO system with a single moving scatterer S^M and K $(k = 1, 2, \ldots, K)$ fixed scatterers S_k^F placed at $(x(t), y(t), z(t))$ and (x_k^F, y_k^F, z_k^F), respectively.

where the LOS and single-bounce scattering components are obstructed. The impact of single-bounce scattering components was previously investigated in [10], [11].

In this work, we will first present the expression for the complex channel gain with a time-variant (TV) path gain and a TV path delay, which will then be used to compute the TV micro-Doppler signatures of the moving object. To validate the proposed trajectory-driven channel model, we consider two experimental scenarios using a single swinging pendulum, where the exact (analytical) TV trajectories of the pendulum are known. For both scenarios, the transmitter antenna is facing the pendulum, whereas the receiver antenna is directed towards the wall and the window for Scenario I and Scenario II, respectively. For additional analysis, we use an inertial measurement unit (IMU) sensor to capture the trajectory of the pendulum. Finally, we compare the micro-Doppler signatures of the moving object computed from the measured RF data with those obtained from the backscattering channel model. The excellent agreement observed between these quantities confirms the validity of the proposed channel model for indoor environments. It also shows that the Doppler properties of moving objects can be accurately extracted solely from the backscattering components. This is of great importance for future smart RF sensing applications, such as reconfigurable intelligent surfaces, Internet of things (IoT) use cases, etc., where the moving objects are not in the field of view of the receiver antennas.

The paper is organized as follows. The 3D geometrical backscattering propagation channel model for indoor environments is described in Section II. The expressions of the complex channel gain and Doppler properties of the proposed channel model is presented in Section III. Section IV provides a comparative analysis of the measurement data and the corresponding numerical results of the trajectory-driven channel model. The conclusion is drawn in Section V.

II. 3D Geometrical Backscattering Model

In this section, we present the 3D geometrical backscattering propagation scenario in an indoor environment as depicted in Fig. 1, where single-input single-output (SISO) system is considered. The transmitter (receiver) antenna is denoted by A^T (A^R) and is placed at the fixed position (x^T, y^T, z^T) $((x^R, y^R, z^R))$ in indoor space. The multipath propagation environment consists of number of fixed objects modelled by K fixed scatterers S_k^F and a single moving object characterized by a single moving scatterer S^M. In Fig. 1, fixed (moving) scatterers are illustrated by black square ■ (red pentagon ⬟). The fixed scatterers are placed at the fixed positions (x_k^F, y_k^F, z_k^F) $(k = 1, 2, \ldots, K)$, where the single moving scatterer has TV coordinates $x(t)$, $y(t)$, and $z(t)$. These TV coordinates are used to define the trajectory $\mathcal{C}(t)$, i.e., $\mathcal{C}(t) = (x(t), y(t), z(t))$, of a moving scatterer. In the model, we consider the impact of backscattering component on the Doppler characteristics of the radio waves.

As illustrated in Fig. 1, the moving scatterer S^M can be described by its relative positions with respect to the transmitter antenna A^T and the fixed scatterer S_k^F by the TV Euclidean distances $d^{T,S^M}(t)$ and $d^{S^M,S_k^F}(t)$, respectively. The TV distances $d^{T,S^M}(t)$ and $d^{S^M,S_k^F}(t)$ are expressed as follows

$$d^{T,S^M}(t) = \sqrt{(x(t) - x^T)^2 + (y(t) - y^T)^2 + (z(t) - z^T)^2} \tag{1}$$

$$d^{S^M,S_k^F}(t) = \sqrt{(x(t) - x_k^F)^2 + (y(t) - y_k^F)^2 + (z(t) - z_k^F)^2}\,. \tag{2}$$

Analogously, the fixed Euclidean distance $d^{S_k^F,R}$ is given by

$$d^{S_k^F,R} = \sqrt{(x_k^F - x^R)^2 + (y_k^F - y^R)^2 + (z_k^F - z^R)^2}\,. \tag{3}$$

In this paper, we investigate the contribution of backscattering components on the Doppler properties of radio signals in the presence of moving objects in indoor environments. For fair analysis, our propagation scenario takes into account horn antennas. These antennas are placed in the environment along a configuration, where single-bounce scattering and line of sight components are blocked. For this reason, we will only consider in our channel model the double-bounce scattering components. In addition, high-pass filtering and mean removal are applied to mitigate the contribution of fixed scatterers (objects) in the room.

III. Micro-Doppler Signature Analysis

This section presents the trajectory-driven SISO channel model for mmWave communication system capturing the mobility of a single point scatterer (object).

A. Complex Channel Gain

We present the expression of the complex channel gain $\mu(t)$ describing the communication link between the transmitter antenna A^T and the receiver antenna A^R. This complex channel gain is obtained form the demodulated radar response $h(t, \tau')$

as defined in [12] over the interval $[0, \tau'_{max}]$, where τ'_{max} is the maximum propagation delay, and it is presented as:

$$\mu(t) = \int_0^{\tau'_{max}} h(t,\tau')d\tau' \quad (4)$$

$$= \frac{c^M(t)}{\pi}\left[\mathrm{Si}\left(\pi B(\tau_{\max} - \tau'^M(t))\right) + \mathrm{Si}\left(\pi B \tau'^M(t)\right)\right] \cdot \exp\left(-j2\pi f_c \tau'^M(t)\right) \quad (5)$$

where $\mathrm{Si}(\cdot)$ stands for the sine integral function [13, Eq. (8.230(1))] and B denotes the frequency bandwidth.

The complex channel gain $\mu(t)$ of the corresponding moving scatterer S^M is characterized by the TV path gains $c^M(t)$, the carrier frequency f_c, and the TV path delay $\tau'^M(t)$. The TV gain $c^M(t)$ is computed according to the free-space path loss model [12], i.e., $c^M(t) = [d^{T,S^M}(t) + d^{S^M,S_k^F}(t) + d^{S_k^F,R}(t)]^{-\gamma/2}$, where $\gamma = 1.7$ denotes the path loss exponent. The TV propagation path delay $\tau'^M(t)$ can be computed by using the trajectory $\mathcal{C}(t) = (x(t), y(t), z(t)))$ of a moving object. This designates the proposed model as trajectory-driven model. Thus, $\tau'^M(t)$ can be expressed in terms of the Euclidean distances $d^{T,S^M}(t)$, $d^{S^M,S_k^F}(t)$, and $d^{S_k^F,R}$ given in (1), (2), and (3), respectively, as follows:

$$\tau'^M(t) = \frac{1}{c_0}\left[d^{T,S^M}(t) + d^{S^M,S_k^F}(t) + D^{S_k^F,R}\right] \quad (6)$$

where c_0 represents the speed of light.

B. Doppler Analysis

In the following, we discuss the Doppler properties of the proposed trajectory-driven backscattering channel model in terms of the TV micro-Doppler signatures (spectrogram) and the TV mean Doppler shift.

The spectrogram of the complex channel gain $\mu(t)$, denoted by $S_\mu(f,t)$, is defined as squared magnitude of the short-time Fourier transform (STFT) of $\mu(t)$, i.e.,

$$S_\mu(f,t) = |X(f,t)|^2 . \quad (7)$$

Here, the STFT $X(f,t)$ is determined according to [14] as

$$X(f,t) = \int_{-\infty}^{\infty} \mu(t) w(t'-t) e^{-i2\pi f t'} dt' \quad (8)$$

where $w(t)$ stands for the positive even window function.

The TV mean Doppler shift $B_\mu^{(1)}(t)$ is then obtained by using the expression of the spectrogram $S_\mu(f,t)$ in (7) as follows

$$B_\mu^{(1)}(t) = \frac{\int_{-\infty}^{\infty} f S_\mu(f,t) df}{\int_{-\infty}^{\infty} S_\mu(f,t) df} . \quad (9)$$

IV. Measurement Campaign and Analysis

This section presents a comparison analysis between the Doppler characteristics computed from the measured RF data and those of the trajectory-driven backscattering channel model. Here, we consider two experiments using a single swinging pendulum as shown in Fig. 2 taking place in a typical laboratory-like room. The size of the laboratory was 11.5 m long, 6 m wide, and 2.5 m high. As shown in Fig. 2, the laboratory room contains several fixed objects (office cabinets, chairs, tables, desktop computers,...) and a single moving object (pendulum). The pendulum is comprised of a ball weighing 3 kg, which is fixed to the ceiling through a cord of length $L = 1.5$ m. According to [11], the analytical expressions of the TV coordinates (displacements) $x(t)$, $y(t)$, and $z(t)$ of the pendulum are given by

$$x(t) = L\sin\left(\arcsin\left(\frac{x_{\max}}{L}\right)\cos\left(\sqrt{\frac{g}{L}}t\right)\right) \quad (10)$$

$$y(t) = 0 \quad (11)$$

$$z(t) = L\left\{1 - \cos\left[\arcsin\left(\frac{x(t)}{L}\right)\right]\right\} \quad (12)$$

where g denotes the gravity acceleration. The symbol $x_{\max}$ stands for the maximum displacement of the pendulum along the $x-$axis and is set to 0.58 m for both experiments. Additionally, for further validation of the proposed trajectory-driven model, we used an IMU sensor, which was fixed to the ball as shown in Fig. 2. This IMU sensor measured the quaternions and linear accelerations of the pendulum and data files were recorded by using a smartphone. The recorded data files were then used to compute the velocities and TV coordinates (trajectories) of the pendulum. Figure 4 illustrates the TV coordinates $x(t)$ and $z(t)$ computed from the analytical (mechanical) model and the IMU data. We can observe an excellent agreement between the TV displacements $x(t)$ and $z(t)$ of the analytical model in (10) and (12) and those of the obtained from the IMU data. In the measurement campaign, we used the Ancortek radar sensor considering a distributed SISO antenna configuration operating at 24 GHz frequency and a bandwidth B =250 MHz. The horn antennas are mounted on tripods of height 1.08 m.

In our experiment, we consider two scenarios for backscattering signal propagation, namely Scenario I and Scenario II. For Scenario I, we consider that the transmitter and receiver antennas are collocated and both are directed in opposite directions. The transmitter is directed towards swinging pendulum, whereas the receiver antenna is directed to the wall as illustrated

TABLE I
MEASUREMENT SETTING PARAMETERS.

Model Parameters	Scenario I	Scenario II
(x^T, y^T, z^T)	(1, 0, 1.08) m	(1, 0, 1.08) m
(x^R, y^R, z^R)	(1, 0, 1.08) m	(1, 0, 1.08) m
(x_k^F, y_k^F, z_k^F)	(6, 0, 1.08) m	(0, -3, 1.08) m
L	1.5 m	1.5 m
$x_{\max}$	0.58 m	0.58 m

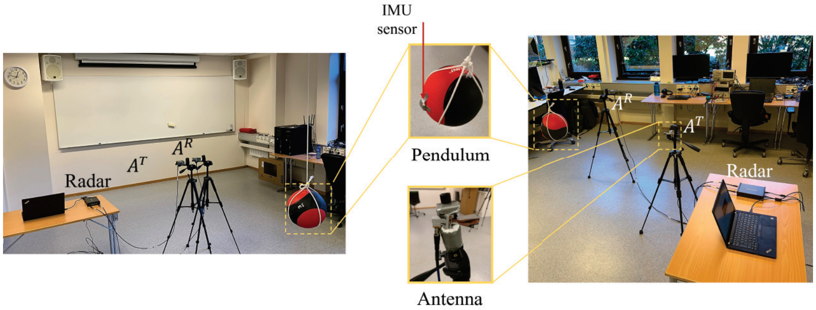

(a) (b)

Fig. 2. Illustration of propagation environment in a laboratory for (a) Scenario I and (b) Scenario II.

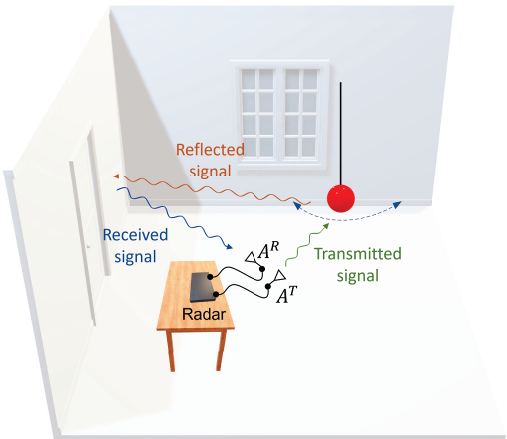

(a)

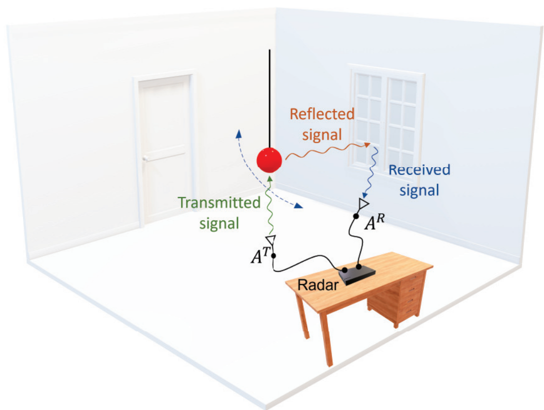

(b)

Fig. 3. Illustration of backscattering propagation for (a) Scenario I and (b) Scenario II.

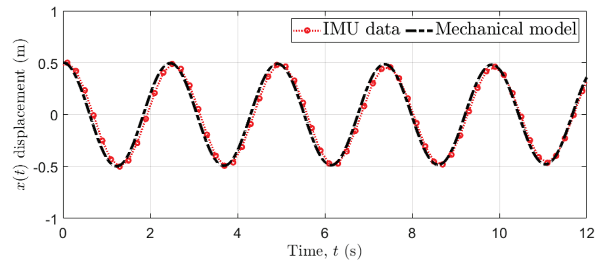

(a)

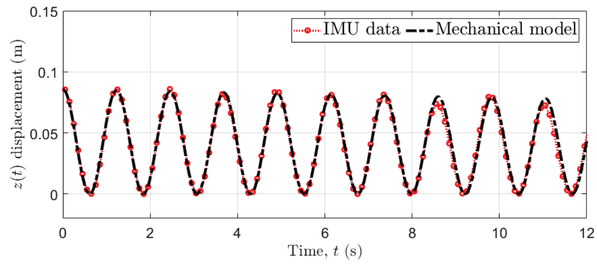

(b)

Fig. 4. The TV (a) $x(t)$ and (b) $z(t)$ displacements of the mechanical model and IMU data.

in Fig. 3a. In Scenario II, the receiver antenna is placed at an angle of 90 degrees w.r.t. the transmitter antenna (see Fig. 2) and is directed towards the window. In this case, the transmitted wave signals will be reflected from the ball to the window and then scattered from the window to the indoor environment to be finally received at the receiver horn antenna as shown in Fig. 3b.

Table I lists up model parameters, such as the length of the rope L, the maximum displacement $x_{\max}$, and the positions of the antennas and reflecting surfaces (fixed scatterers for double-bounce scattering) for both scenarios.

Figure 5 illustrates the spectrograms of the measured and simulated SISO channels for Scenario I. In Figs. 5a, 5b, and 5c we can observe an excellent match between the spectrograms computed from the measured RF channel and those obtained form the backscattering trajectory-driven channel model using analytical (mechanical) and IMU-based trajectories, respectively. Analogously, the spectrograms of the measured and simulated SISO channels for Scenario II are shown in Fig. 6. In this result, we can see the impact of the travelling distance on the spectrograms in the frequency range. For further analysis, we also investigated the TV mean Doppler shift for both scenarios. The good fit observed in Fig. 7 for both scenarios demonstrates the validity of the proposed backscattering trajectory-driven channel model.

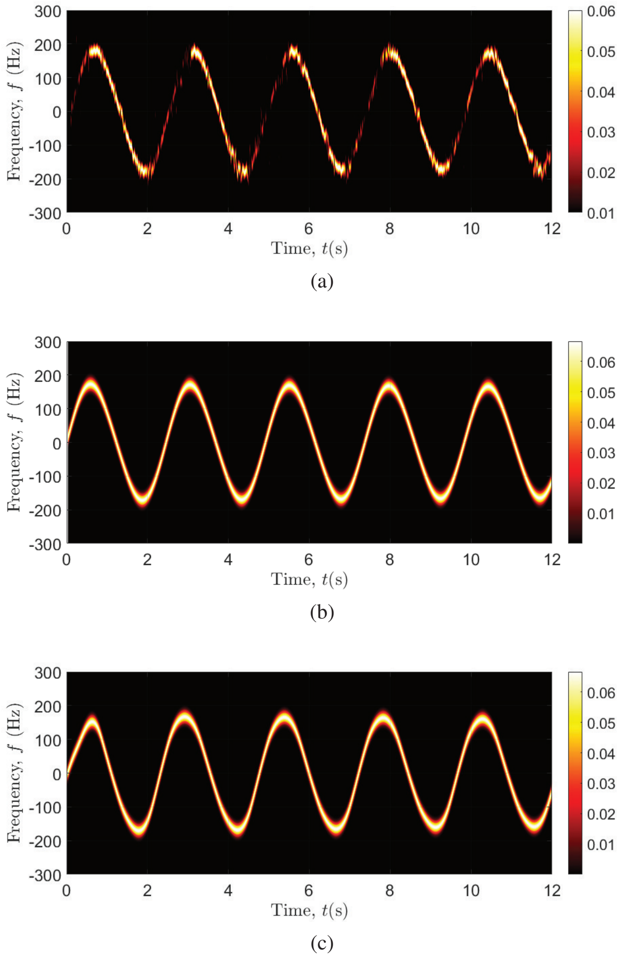

Fig. 5. Illustrations of the spectrograms $\hat{S}_\mu(f,t)$, $S_\mu(f,t)$, and $\tilde{S}_\mu(f,t)$ of the (a) measured radar data, (b) analytical (mechanical) channel model, and (c) IMU-based channel model, respectively, for Scenario I.

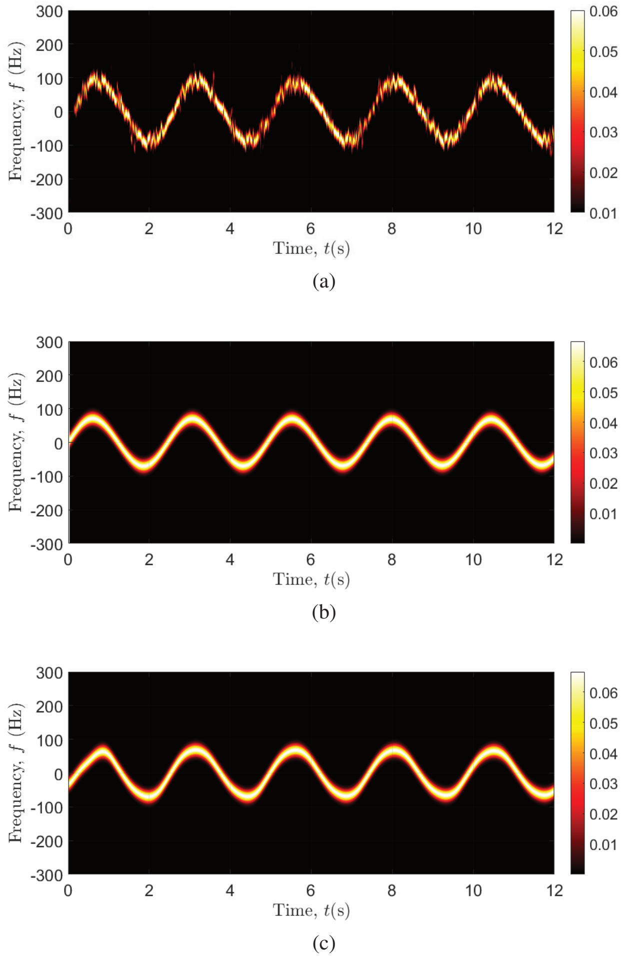

Fig. 6. Illustrations of the spectrograms $\hat{S}_\mu(f,t)$, $S_\mu(f,t)$, and $\tilde{S}_\mu(f,t)$ of the (a) measured radar data, (b) analytical (mechanical) channel model, and (c) IMU-based channel model, respectively, for Scenario II.

V. Conclusion

In this paper, we proposed a backscattering trajectory-driven non-stationary mmWave indoor channel model in the presence of a single moving object (modelled by a single point scatterer) considering a distributed SISO communication system. We presented the expressions of the complex channel gain and the Doppler properties (in terms of the spectrogram and the TV mean Doppler shift) of the proposed backscattering channel model. To capture the mobility of the single scatterer (object), a measurement campaigns was carried out in a laboratory room by using a mmWave radar system working in the 24 GHz frequency band. The validity of the proposed channel model is confirmed by the excellent match, which can be observed between the micro-Doppler signatures of the swinging pendulum computed from the real-world measured RF data and those obtained from the trajectory-driven channel model. These results confirm the importance of considering backscattering phenomena for future RF sensing technologies, especially targeting indoor applications.

References

[1] S. Kishimoto, M. Kim, D. He, and K. Guan, “Scattering process identification and cluster analysis for millimeter-wave indoor channel model,” in *2018 International Symposium on Antennas and Propagation (ISAP)*, 2018, pp. 1–2.

[2] W. Zhao, G. Wang, S. Atapattu, T. A. Tsiftsis, and X. Ma, “Performance analysis of large intelligent surface aided backscatter communication systems,” *IEEE Wireless Communications Letters*, vol. 9, no. 7, pp. 962–966, 2020.

[3] I. Cnaan-On, S. J. Thomas, J. L. Krolik, and M. S. Reynolds, “Multichannel backscatter communication and ranging for distributed sensing with an FMCW radar,” *IEEE Transactions on Microwave Theory and Techniques*, vol. 63, no. 7, pp. 2375–2383, 2015.

[4] A. Guerra, F. Guidi, A. Clemente, R. D’Errico, and D. Dardari, “Delay spread characterization of millimeter-wave indoor backscattering channel,” in *2016 10th European Conference on Antennas and Propagation (EuCAP)*, 2016, pp. 1–2.

[5] J. Pascual-García, J.-M. Molina-García-Pardo, M.-T. Martínez-Inglés, J.-V. Rodríguez, and N. Saurín-Serrano, “On the importance of diffuse scattering model parameterization in indoor wireless channels at mm-wave frequencies,” *IEEE Access*, vol. 4, pp. 688–701, 2016.

[6] Y.-H. Kim, C. Yoon, H.-S. Ahn, and S.-o. Lim, “Implementation of multi-level modulated-backscatter communication system using ambient Wi-Fi signal,” in *2019 IEEE International Conference on RFID Technology and Applications (RFID-TA)*, 2019, pp. 476–479.

[7] Y. Zhang, F. Gao, L. Fan, X. Lei, and G. K. Karagiannidis, “Backscatter

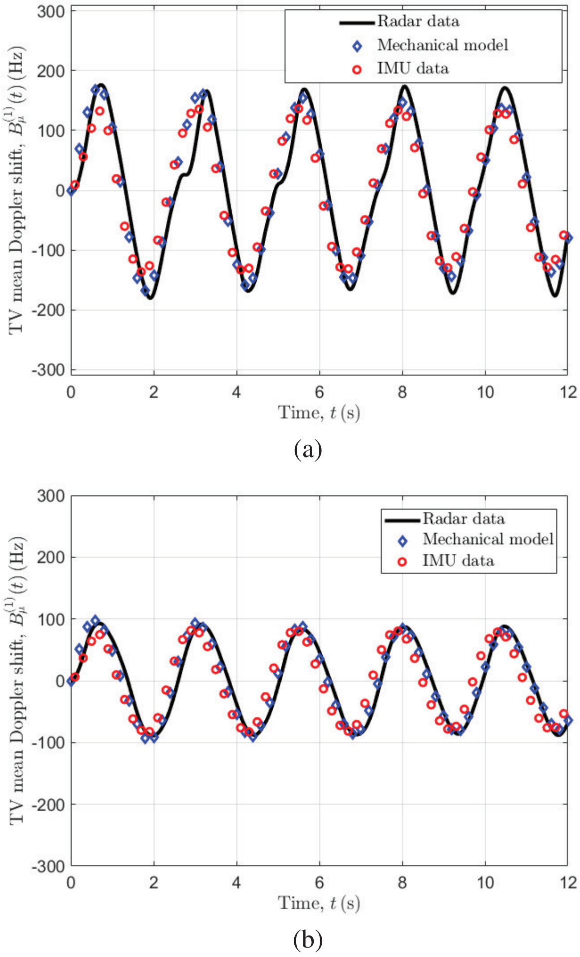

Fig. 7. The TV mean Doppler shift for (a) Scenario I and (b) Scenario II, respectively.

communications over correlated Nakagami-m fading channels," *IEEE Transactions on Communications*, vol. 67, no. 2, pp. 1693–1704, 2019.

[8] R. Valentini, P. D. Marco, R. Alesii, and F. Santucci, "Cross-layer analysis of distributed passive RFID systems over faded backscattering links," in *2020 IEEE Wireless Communications and Networking Conference (WCNC)*, 2020, pp. 1–6.

[9] Z. Luo, Q. Zhang, W. Wang, and T. Jiang, "Single-antenna device-to-device localization in smart environments with backscatter," *IEEE Internet of Things Journal*, vol. 9, no. 12, pp. 10 121–10 129, 2022.

[10] N. Avazov, R. Hicheri, and M. Pätzold, "A trajectory-driven SIMO mm-Wave channel model for a moving point scatterer," in *15th European Conference on Antennas and Propagation (EuCAP)*, 2021, pp. 1–5.

[11] N. Avazov, R. Hicheri, M. Muaaz, F. Sanfilippo, and M. Pätzold, "A trajectory-driven 3D non-stationary mm-wave MIMO channel model for a single moving point scatterer," *IEEE Access*, vol. 9, pp. 115 990–116 001, 2021.

[12] R. Hicheri, N. Avazov, M. Muaaz, and M. Pätzold, "The transfer function of non-stationary indoor channels and its relationship to system functions of LFMCW radars," in *IEEE 22nd International Workshop on Signal Processing Advances in Wireless Communications (SPAWC)*, 2021, pp. 151–155.

[13] I. S. Gradshteyn and I. M. Ryzhik, *Table of integrals, series, and products*. Academic press, 2007.

[14] N. Avazov, R. Hicheri, and M. Pätzold, "A trajectory-driven SISO mm-wave channel model for a human activity recognition," in *2021 17th International Conference on Wireless and Mobile Computing, Networking and Communications (WiMob)*, 2021, pp. 133–138.